• Clinical Research •

Dynamic changes of spontaneous brain activity in patients after LASIK: a resting-state fMRI study

Hui Zhang[1], Zi-Song Xu[2], Jin-Yu Hu[2], Zhen-Zhe Liu[2], Lei Zhong[3], Liang-Qi He[2], Cheng Chen[2], Xiao-Yu Wang[2], Hong Wei[2], Yan-Mei Zeng[2], Qian Ling[2], Xu Chen[4], Yi-Xin Wang[5], Yi Shao[3]

[1]Nanchang Bright Eye Hospital, Nanchang 330000, Jiangxi Province, China
[2]Department of Ophthalmology, the First Affiliated Hospital, Jiangxi Medical College, Nanchang University, Nanchang 330006, Jiangxi Province, China
[3]Department of Ophthalmology, Shanghai General Hospital, Shanghai Jiao Tong University School of Medicine; National Clinical Research Center for Eye Diseases, Shanghai Key Laboratory of Ocular Fundus Diseases, Shanghai Engineering Center for Visual Science and Photomedicine, Shanghai Engineering Center for Precise Diagnosis and Treatment of Eye Diseases, Shanghai 200080, China
[4]Ophthalmology Centre of Maastricht University, Maastricht 6200MS, Limburg Provincie, the Netherlands
[5]School of Optometry and Vision Science, Cardiff University, Cardiff, CF24 4HQ, Wales, UK
Co-first authors: Hui Zhang and Zi-Song Xu
Correspondence to: Yi Shao. Department of Ophthalmology, Shanghai General Hospital, Shanghai Jiao Tong University School of Medicine, Shanghai 200030, China. freebee99@163.com; Yi-Xin Wang. School of Optometry and Vision Science, Cardiff University, Cardiff, CF24 4HQ, Wales, UK. 731579475@qq.com
Received: 2023-11-19 Accepted: 2024-09-05

Abstract

● **AIM:** To investigate changes in local brain activity after laser assisted *in situ* keratomileusis (LASIK) in myopia patients, and further explore whether post-LASIK (POL) patients and healthy controls (HCs) can be distinguished by differences in dynamic amplitude of low-frequency fluctuations (dALFF) in specific brain regions.

● **METHODS:** The resting-state functional magnetic resonance imaging (rs-fMRI) data were collected from 15 myopic patients who underwent LASIK and 15 matched healthy controls. This method was selected to calculate the corresponding dALFF values of each participant, to compare dALFF between the groups and to determine whether dALFF distinguishes reliably between myopic patients after LASIK and HCs using the linear support vector machine (SVM) permutation test (5000 repetitions).

● **RESULTS:** dALFF was lower in POL than in HCs at the right precentral gyrus and right insula. Classification accuracy of the SVM was 89.1% (P<0.001).

● **CONCLUSION:** The activity of spontaneous neurons in the right precentral gyrus and right insula of myopic patients change significantly after LASIK. SVM can correctly classify POL patients and HCs based on dALFF differences.

● **KEYWORDS:** laser assisted *in situ* keratomileusis; resting-state functional magnetic resonance imaging; dynamic brain activity; amplitude of low-frequency fluctuations; support vector machine

DOI:10.18240/ijo.2025.03.16

Citation: Zhang H, Xu ZS, Hu JY, Liu ZZ, Zhong L, He LQ, Chen C, Wang XY, Wei H, Zeng YM, Ling Q, Chen X, Wang YX, Shao Y. Dynamic changes of spontaneous brain activity in patients after LASIK surgery: a resting-state fMRI study. *Int J Ophthalmol* 2025;18(3):487-495

INTRODUCTION

Myopia is a form of ametropia[1]. When the myopic eye is relaxed, parallel light from the visual scene enters the eye, is refracted and focused in front of the retina, resulting in a blurred image on the retina[2]. The clinical definition of high myopia is ametropia at least 6.00 diopters (D) or an axial length of at least 26 mm[3]. In recent years, the prevalence of myopia has increased[4-5], with significant impact in adolescents[6]. Many countries have published reports that the population with myopia has increased, including the United States[7], Europe[8], and Denmark[9], and the myopia growth rate in many East and South Asian countries is particularly apparent[10]. Myopia has become one of the most common ophthalmic diseases[2], and can cause related ocular complications[11-12], which increase the risk of eye diseases such as cataract, glaucoma, retinal detachment and myopic macular degeneration, leading to blindness[13]. According to previous studies, high myopia is one of the main causes of global vision loss, and is highly heritable[14], such that a child whose parents are both myopic has a significantly increased risk of myopia[15-18]. In addition to

genetic factors, risk factors for myopia include lifestyle, diet, environment, close work, reduced time outdoors, and a high ratio between close work and outdoor activity[6], such as more close working hours, shorter outdoor time, and greater close working/outdoor ratio may lead to a higher risk of myopia[19]. Although myopia is not an organic disease, it will seriously affect patients' quality of life, causing irreversible visual loss if allowed to develop[6]. Therefore, the prevention and treatment of myopia has become an urgent global public health problem.

With the improvement of living standards and health requirements, patients increasingly address their myopia by refractive surgery to remove the need for glasses. In recent years, interest in corneal refractive surgery has gradually increased. Laser assisted *in situ* keratomileusis (LASIK) is a globally recognized refractive surgery with good safety and effectiveness, and has become one of the most common operations in clinic[20-21]. The principle of this operation is to make a corneal flap using a mechanical corneal lamellar knife, lift the flap and use laser to change the curvature of the anterior corneal surface[2]. Although clinical practice has shown that LASIK is efficient, stable and safe[21], there are still some risk factors. For example, the operation may lead to corneal flap dissociation, dry eye discomfort, diffuse keratitis or refractive regression. According to previous studies, almost all patients will experience dry eye symptoms immediately after the operation. Three months later[22-25], only 28% of patients report dry eye[26].

Resting-state functional magnetic resonance imaging (rs-fMRI) is a functional brain imaging technology[27-30], which provides information about spontaneous brain activity non-invasively. Amplitude of low-frequency fluctuation (ALFF) evaluates the intensity of local spontaneous neural activity by observing the fluctuation of low-frequency blood oxygen level-dependent (BOLD) signals in the resting state. ALFF measurement is a reliable and effective tool, which can be used to analyze fMRI data when the brain is not undertaking a specific task[28]. In recent years, ALFF technology has been widely used to investigate the brain activity of a variety of eye diseases[31]. Previous studies have found abnormal ALFF in many brain regions of patients with high myopia, and this abnormality is considered an important feature of visual dysfunction[32]. These studies have provided convincing data through resting state ALFF measurement, demonstrating that extensive brain regions are involved in high myopia. However, they are limited since the analysis of ALFF data in the resting state does not consider the dynamic characteristics of brain activity during the data collection period. This problem can be addressed by ALFF technology combined with the "sliding window" method. This approach can not only detect satisfactory dynamic functional connection features, but also has high accuracy and sensitivity compared with static methods[33-37]. The dynamic amplitude of low-frequency fluctuation (dALFF) analysis method is a new way to study local neuronal activity, and is a major breakthrough in the exploration of human brain activity. It is a powerful supplement to static analysis of the functional organization and information function of the brain, and provides a more comprehensive understanding of variations in brain activity and of brain function. In the present study, we adopted this approach and used a support vector machine (SVM) to determine whether myopic patients after LASIK can be distinguished from controls on the basis of their dALFF levels. The SVM is a generalized linear classifier for binary classification of data by supervised learning. Its high accuracy of classification and prediction has made SVM one of the most popular supervised machine learning technologies[38-40]. To our knowledge, this study is the first to use dALFF combined with SVM to explore brain neural activity changes in patients after LASIK and in controls. In this study, the experimental group includes patients who have undergone LASIK surgery, and the control group includes healthy control subjects. It can be speculated that abnormal ALFF values in some brain regions may be found in patients after LASIK, may be used as a basis for evaluating the outcome and completion of LASIK, and provide clues for further predicting the level of postoperative visual acuity.

PARTICIPANTS AND METHODS

Ethical Approval The study methods and protocols were approved by the Medical Ethics Committee of the First Affiliated Hospital of Nanchang University (Nanchang, China) and followed the principles of the Declaration of Helsinki. All subjects were notified of the objectives and content of the study and latent risks, and then provided written informed consent to participate.

Participants In this prospective study 15 patients (6 males and 9 females) with high myopia who underwent LASIK surgery at the First Affiliated Hospital of Nanchang University were randomly selected as the post-laser assisted *in situ* keratomileusis (POL) group, and 15 people without other eye diseases were selected as the healthy control group. The baseline characteristics (age, gender, and education level) of the two groups were comparable. POL patients were included according to the following criteria: 1) older than 18y; 2) patients required corneal refractive surgery to improve refractive status and had reasonable expectations of the operation; 3) no active ocular lesions, no history of trauma, serious systemic diseases or psychological diseases; 4) best corrected visual acuity (BCVA) ≥0.8 preoperatively, and the refractive error in diopters did not increase significantly within two years (increase ≤0.50 D); 5) spherical refractive error -6.00 to -10.00 D, and cylindrical error <-3.00 D; 6) soft contact

lens, hard contact lens and corneal shaping lens were not worn for at least 1wk, 1, and 3mo respectively prior to surgery. There is only one variable between the myopia patients and healthy controls, so there will be no statistic difference. The exclusion criteria were 1) keratoconus, glaucoma, cataract affecting eyesight, retinitis pigmentosa, retinal detachment, severe dry eye, abnormalities of ocular movements, ocular active inflammation or serious ocular appendage lesions (eyelid defect or deformity); 2) amblyopia; 3) scotopic pupil diameter >7.5 mm; 4) central corneal thickness ≤450 μm; expected residual corneal thickness after incision <280 μm and <50% of preoperative corneal thickness; 5) diabetes, immune and collagenous diseases, scar constitution and other diseases that affect postoperative healing; 6) suffering from mental illness such as anxiety or depression.

Magnetic Resonance Imaging Parameters A 3.0 T MRI scanner was required to obtain MRI data of all subjects. Before the MRI scan, each participant was advised by the researchers that they must close their eyes and not have any tension during the operation, so as to make the brain and body in a natural and relaxed state. To avoid possible head movements, we choose to place some comfortable and soft belts and foam pads around the head to stabilize the head. In addition, the researchers also equipped each subject with earplugs to protect them from the noise generated during MRI scanning. During the whole operation, the following parameters are selected to obtain RS fMRI data: repetition time (TR) =2000 ms, echo time (TE)= 40ms, flip angle=90°, slice thickness/gap=4.0/1 mm, field of view (FOV)=240 mm×240 mm, in- plane resolution=64×64, 30 axial slices covering the whole brain, and 240 volumes acquired in 8min. In addition, we acquired high-resolution brain structural images for each subject by using a T1-weighted 3D MP-RAGE sequence (TR=1900ms, TE=2.26ms, flip angle=9°, matrix=256×256, FOV=240 mm×240 mm, thickness=1.0 mm, and 176 sagittal slices).

Functional Magnetic Resonance Imaging Data Preprocessing This study refers to the method of a previous research[41] and uses the same software and method to process and analyze rs-fMRI data. Since the subjects may not adapt to the scanning conditions at the beginning of the scanning, in order to ensure that all images are obtained when the subject is in a stable state, it is necessary to discard the images obtained at the first ten time points, and then slice all the remaining images to correct the time difference. In addition, it is also necessary to correct the head movement to normalize the spatial position, in all data, only the images of subjects whose head movement translation is less than 2.0 mm and rotation movement is less than 2.0° can enter the subsequent analysis. Then, the processed image is subjected to 6 mm full width half height Gaussian kernel spatial smoothing, band-pass filtering (0.01 Hz <frequency <0.08 Hz) and de-linear drift. Due to the inevitable potential impact of head motion, several variables need to be introduced for regression analysis, including six head motion parameters, cerebrospinal fluid signal and white matter signal. Next, the image is normalized to the standard echo-planar images (EPI) template and resampled to a voxel size of 3×3×3 mm^3 to meet the spatial standards of the Montreal Institute of Neurology (MNI).

Dynamic Amplitude of Low-Frequency Fluctuation Analysis Dynamic amplitude low frequency fluctuation (dALFF) analysis is carried out in the time domain dynamic analysis (TDA) toolkit based on DPABI[34]. In order to improve the accuracy of dALFF calculation, fMRI images were band-pass filtered (0.01-0.08 Hz). Sliding window method is the key technology of dALFF compared with ALFF. It is a good choice to capture potential functional related dynamic phenomena between brain regions. In this method, a fixed length time window is selected, that is, the window length. The data in the whole scanned time period is divided into several sub time periods according to the length of the time window, and the time points in a window are respectively used to calculate the time, and the corresponding functional connections in the time window. Then move the window in time by a fixed amount of time point (ranging from one time point to the length of the whole scanning time point), which is called step size. This period of time point defines the amount of overlap between continuous windows. This sliding process results in quantifying the time-varying behavior of brain activity and functional connections during scanning. Window length and step size are two attributes of sliding window and important parameters for dynamic analysis. The selected window width and step size must ensure that a sufficient number of time points are collected to facilitate reliable calculation. Li *et al*[33] and Zalesky and Breakspear[42] demonstrated that the window length range of 10-75TR (step=1 TR) meets the standard. In this study, the window length of 30TR (step=1 TR) is used to calculate ALFF for each sliding window. In order to evaluate the difference of ALFF, the standard deviation (SD) of ALFF value per voxel in each window must be calculated.

Statistical Analysis SPSS16.0 (SPSS Inc., Chicago, IL, USA) was used as a statistical analysis tool to compare demographic and clinical data between patients after LASIK and healthy controls. The difference between sex-based groups was observed by Chi-square test, and the difference between age-based groups was observed by two-sample *t*-test. Average age and sex were used as covariates to compare the difference of dALFF/ALFF between the LASIK group and hc group using general linear model (GLM). Multiple comparisons were corrected appling Gaussian Random-Field (GRF) method (voxel level, $P<0.01$; Clustering level, $P<0.05$).

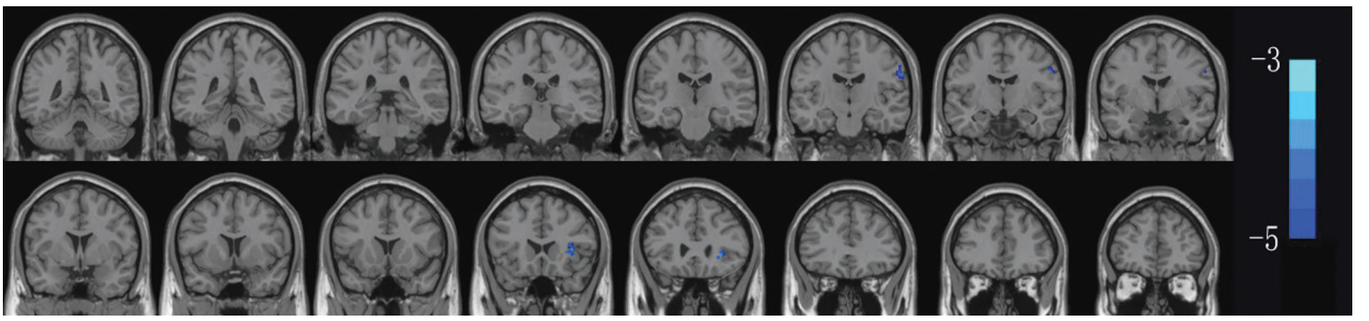

Figure 1 The dALFF of R insula and R precentral gyrus decreased in cross section.

Table 1 Basic information of different groups

Parameters	HCs	POL	*t*	*P*
Male/female	9/6	9/6	N/A	>0.99
Age (y)	21.58±1.55	21.82±2.92	1.247	0.945
Duration (y)	N/A	7.68±2.64	N/A	N/A
SE-L (D)	-0.75±0.15	-0.55±0.10	0.984	0.895
SE-R (D)	-0.50±0.10	-0.50±0.15	1.176	0.929
Astigmatism-L (D)	-0.25±0.10	-0.15±0.15	1.023	0.907
Astigmatism-R (D)	-0.15±0.15	-0.15±0.10	1.086	0.981
Color vision	15R	15R	N/A	>0.99
Confrontation vision field	15R	15R	N/A	>0.99

HCs: Healthy controls; L: Left; POL: Post-LASIK, N/A: Not applicable; R: Right; SE: Spherical equivalent; LASIK: Laser assisted *in situ* keratomileusis.

Table 2 dALFF differences between HCs and POL patients

Brain area	Brodmann area	Voxel	MNI coordinates of peak voxel			*t*
			X	Y	Z	
POL<HCs						
R insula	13	28	30	27	0	-4.1247
R precentral gyrus		27	60	-15	30	-3.7518

dALFF: Dynamic amplitude of low-frequency fluctuations; HCs: Healthy controls; POL: Post-LASIK; R: Right; MNI: Montreal neurological institute; LASIK: Laser assisted *in situ* keratomileusis.

Support Vector Machine Analysis Dynamic ALFF levels were used to classify data. Some of the classified data were imported to the SVM for machine learning. To minimize the limitation of the small sample size, cross validation was achieved in a permutation test with 5000 repetitions. In each permutation, the characteristics of HCs and POL patients were randomly reassigned, and the SVM repeated the classification process. Once all permutations had been processed, the *P* value was calculated.

RESULTS

Demographics and Clinical Data The age, weight, height and monocular refractive errors of the two groups were similar. More details can be found in Table 1.

Differences in ALFF/dALFF A significant difference in dALFF was found between the two groups, as shown in Figure 1 and Table 2 with significantly lower values in the right insula and right precentral gyrus in patients with high myopia POL compared with HCs.

Classification Results Figure 2 showed the results of classification. The linear SVM classifier using Leave-One-Out-Cross-Validation (LOOCV) achieved an accuracy of 89.1%, sensitivity of 94.4%, and specificity of 89.4% (P<0.001). The receiver operating characteristic (ROC) curve of the classifier was 0.9766.

Correlation Analysis A significant negative linear correlation was found between dALFF of the right insula and anxiety or depression in patients after LASIK (Figure 3).

DISCUSSION

Few studies have used SVM technology to distinguish the characteristics of spontaneous brain activity in patients with high myopia after LASIK from the perspective of dynamic ALFF. While some scholars have in recent years used resting-state fMRI to study neuronal after LASIK surgery (Table 3)[43-44], our research is the first to combine dALFF with SVM. The present study shows that the dALFF values of the right precentral gyrus and right insula in patients with high myopia after LASIK are lower than those of HCs (Figure 4), and that reduced dALFF values in these two regions can be used as

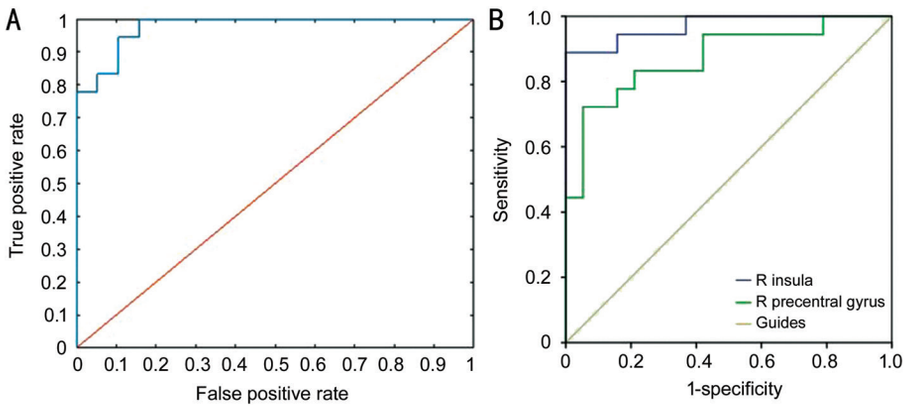

Figure 2 ROC curve analysis of the mean dynamic ALFF values for altered brain regions A: The classification accuracy of dynamic ALFF changes of R precentral gyrus and R insula in LASIK group was obtained by leaving one cross validation method; B: ROC curve analysis of the mean dALFF values for altered brain regions. The area under the ROC curve were 0.971 (P<0.0001; 95%CI: 0.923-1.000) for R insula; R precentral gyrus 0.874 (P<0.0001; 95%CI: 0.758-0.990). dALFF: Dynamic amplitude of low-frequency fluctuation; R: Right; AUC: Area under the curve; ROC: Receiver operating characteristic curve.

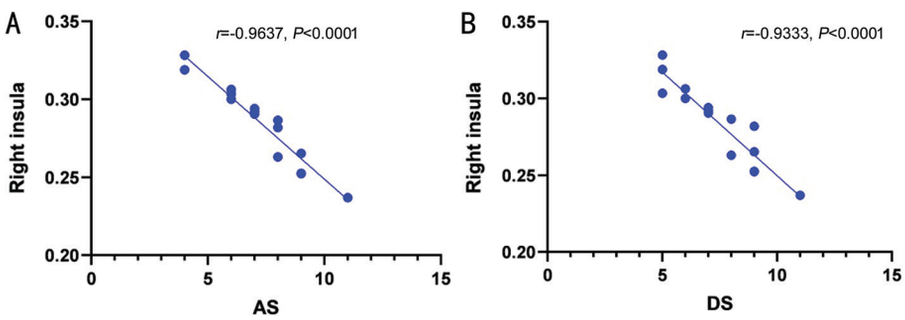

Figure 3 Correlation analysis between dALFF values of right Insula and the clinical behaviors A: The anxiety score was negatively correlated with dALFF values (r=−0.9637, P<0.0001); B: The depression scores was negatively correlated with dALFF values (r=-0.9333, P<0.0001). dALFF: Dynamic amplitude of low-frequency fluctuation; AS: Anxiety scores; DS: Depression scores.

classification markers to distinguish patients who underwent LASIK from HCs.

Previous research indicates extensive regional abnormalities in brain static neuronal activity in patients with high myopia (Table 4)[45-46]. Experiments by Huang *et al*[32], Guo *et al*[47], and Chen *et al*[48] in these patients show reduced ALFF values in the bilateral frontal lobe, middle temporal gyrus, insular lobe, right inferior parietal lobule and left occipital lobe, and significantly increased ALFF values in the left caudate nucleus, left central posterior gyrus, left wedge lobe, left inferior parietal lobule and thalamus. Less recent research compared spontaneous neuronal brain activity in patients with high myopia before and after LASIK. They found that after LASIK ALFF values decreased significantly in the left superior marginal gyrus and the right inferior frontal triangle gyrus and increased in the left parahippocampal gyrus, cerebellar vermis and left posterior cingulate cortex[2]. It is interesting to note that abnormalities were limited to the right insula in the present study, with no indication of the abnormalities reported previously and summarized above in patients treated with LASIK compared with controls, providing evidence of the high effectiveness and reliability of LASIK. In addition, however,

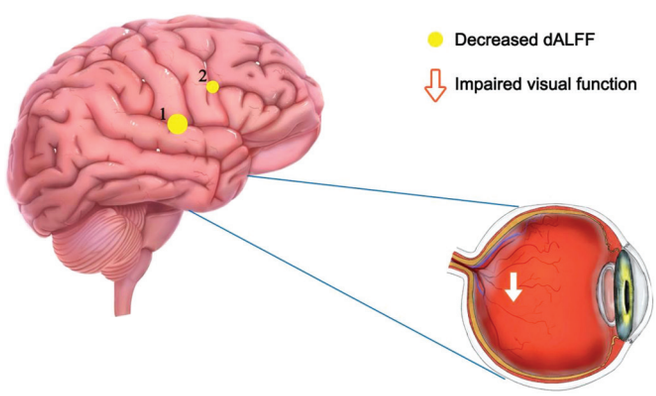

Figure 4 The mean dALFF values of altered brain regions Compared with the HCs, the dALFF values of the following regions were decreased to various extents: 1- R insula (t=-4.1247), 2- R precentral gyrus (BA 40, t=-3.7518). dALFF: Dynamic amplitude of low-frequency fluctuation; HCs: Healthy controls; BA: Brodmann's area.

decreased dALFF values were found in the right precentral gyrus, an area not previously found to show abnormal activity in this group, and perhaps suggesting an adverse effect of LASIK on the right precentral gyrus.

The precentral gyrus is located in the frontal lobe of the cerebral cortex[49], between the central sulcus and the central

Table 3 Resting-state fMRI studies on patients after LASIK surgery

Author	Year	Method	Conclusion
Yu *et al*[2]	2020	ALFF	There were significant fluctuations of ALFF values in specific brain areas between the same patients before and after Lasik surgery
Malecaze *et al*[43]	2001	fMRI	Abnormal activation of visual cortex occurred in patients after LASIK
Vuori *et al*[44]	2011	mffMRI	Refractive surgery (including LASIK) in anisometropic adult patients induce plastic changes in primary visual cortex

LASIK: Laser assisted *in situ* keratomileusis; ALFF: Amplitude of low-frequency fluctuations; fMRI: Functional magnetic resonance imaging; mffMRI: Multifocal functional magnetic resonance imaging.

Table 4 Rs-MRI method applied in myopia patients in the current literatures

Author	Year	Method	Abnormal brain areas	
			Decreased values	Increased values
Guo *et al*[47]	2010	ALFF	frontal lobe, R IPL	LCN, thalamus, occipital lobe
Huang *et al*[32]	2016	ALFF	MTG, IFG, R IPL	MCC, L IPL
Hu *et al*[45]	2018	DC	R IFG, R MFG, R SMG, R IPL	L PreCG, L PosCG, R CPL, R MCG
Zhai *et al*[46]	2016	FCD	Short-range FCD: R PCC/preCun; L PCC/preCun; Long-range FCD: R PCC/preCun; L ITG; R SMG; R rlPFC	-

IPL: Inferior parietal lobule; LCN: Left caudate nucleus; MTG: Middle temporal gyrus; IFG: Inferior frontal gyrus; MCC: Midcingulate cortex; MFG: Middle frontal gyrus; SMG: Supramarginal gyrus; PreCG: Precentral gyrus; PosCG: Postcentral gyrus; CPL: Cerebellum posterior lobe; MCG: Middle cingulate gyrus; PCC: Posterior cingulate cortex; preCun: Precuneus; ITG: Inferior temporal gyrus; rlPFC: Rostrolateral prefrontal cortex; R: Right; L: left.

anterior sulcus which is parallel to the central sulcus on the ascending side of the frontal lobe. The precentral gyrus is an important structure of the frontal lobe, and contains numerous giant pyramidal cells. The fibers emitted by pyramidal cells in this area form a pyramidal system, terminating in the motor cells of the anterior horn of the spinal cord. Therefore, the precentral gyrus is the motor center, containing many motor nerve fibers and its function is closely related to motor preparation and execution. It controls the fine random movement of the contralateral half of the body (so right precentral gyrus injury may cause left hemiplegia, and vice versa) and is the origin of the corticospinal and corticomedullary tracts. Some proprioceptive fibers also project to the precentral gyrus[50-51]. In addition, injury of the left precentral gyrus can reportedly lead to isolated nerve paralysis[52], foreign accent syndrome[53], motor aphasia[54] and other harmful effects. Therefore, the abnormal decrease of dALFF values in the right precentral gyrus after LASIK is a reminder of the need to track the health status of patients after LASIK and to pay attention to the possible adverse reactions. The precentral gyrus belongs to the primary motor area and is involved in processing of a variety of motor function signals including not only neural circuits with the spinal cord, pons and thalamus, but also multiple complex circuits with the auxiliary motor area in the motor cortex. Functional connections between the anterior central gyrus and the limbic lobe, basal ganglia, cerebellum, parietal lobe, frontal lobe and other brain regions may help to explain the decrease of dALFF values in the right precentral gyrus after LASIK.

The insula is located in the deep part of the lateral fissure of the brain and is covered by the frontal lobe, temporal lobe and parietal lobe[55]. The central sulcus of insula divides the insula into anterior and posterior regions[56-57]. The anterior insula forms the limbic system together with the marginal lobe, amygdala, anterior thalamic nucleus, hypothalamus, midbrain tegmental, frontal orbital surface and other structures, is widely connected with reticular structure and cerebral cortex, and is adjacent to the important primary auditory center, language center and basifacial sensory and motor areas[58]. It is worth noting that the insula has extensive nerve fiber connections with surrounding structures so its functions are complex, synthesizing and connecting diversified information in the brain. It has relay station-like role and participates in processing visceral sensation, visceral movement, vestibular sensation, attention, pain, emotion, language, movement, music, diet and other related information. Its function is also related to taste, vision, smell, hearing and touch[59]. The insula has four network structure regions: middle posterior, anterior ventral, anterior dorsal and central regions, which are related to motor sensation, social emotion, cognition, smell and taste respectively. A previous study showed that the anterior insula is an important part of social emotion[60]. The anterior ventral and anterior base of the insula play important roles in the generation and regulation of emotion. The anterior base of the insula may be related to empathy[61]. It plays a connecting role between emotional processing and mirror nervous system, senses the pain feelings of others, and enables itself to match the painful feelings of the observed object. In addition, the insula may participate in regulation of autonomic nervous system function[62]. The right insula mainly regulates sympathetic nerve function, and its injury diminishes activity of this system as well as emotion, resulting in reduced

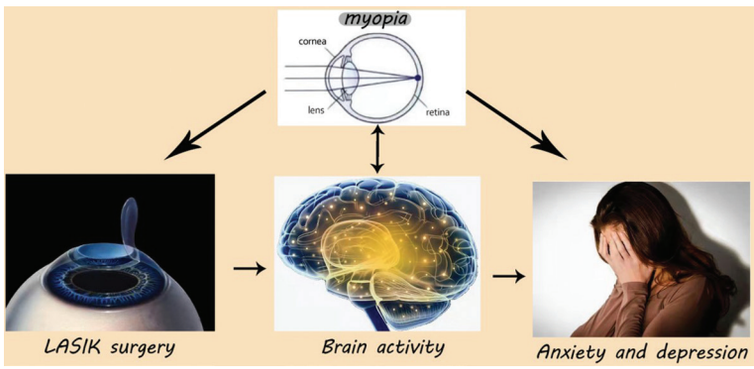

Figure 5 The relationship between changes in internal eye states and vision, brain activity, and emotional state.

Table 5 Brain areas with changed dALFF values and the potential impacts

Brain areas	Experimental result	Brain function	Anticipated results
R insula	LASIK<HC	Social emotion, cognition, motor sensation, taste and smell	Depression, mood disorder, schizophrenia
R precentral gyrus	LASIK<HC	Motor control	Hypoactivity of this region

dALFF: Dynamic amplitude of a low-frequency fluctuation; R: Right; LASIK: Laser assisted *in situ* keratomileusis; HC: Healthy control.

allergic response and decline of willpower and action[63-64]. Previously, positron emission tomography (PET) and fMRI studies suggested that the insula was involved in the course of mental illness[65] such as mood, panic, obsessive-compulsive and post-traumatic stress disorders and schizophrenia. Li *et al*[66], Lanzenberger *et al*[67], and Su *et al*[68] found significantly altered morphology and metabolism of the cerebral insula in patients with depression. The correlation between HADS score and dALFF value of the right insula in patients after LASIK in the present study suggests that LASIK has not improved mood (anxiety and depression) and indicates a need for awareness of postoperative emotional changes in patients and for prevention of harmful outcomes such as depression, cognitive impairment and neurasthenia (Figure 5).

In general, our results verify that the sliding window-based dynamic ALFF method can be used to describe the dynamic functional separation of brain networks, and has high sensitivity to altered spontaneous neural activities. In addition, we found fluctuations in dALFF values in specific brain regions of POL patients, providing an indicator for prediction of postoperative recovery level in patients, and suggesting a need to prevent potential adverse events that may occur after LASIK (Table 5).

However, our study has some limitations. For example: 1) the small sample size may affect accuracy of the results; 2) other factors, such as the patient's own health status, preoperative myopia and the length of the disease course, will affect the patient's recovery level and variance in these factors increase the uncertainty of the results. Despite its limitations, our study detected changes in local brain activity after LASIK. In future research, we will optimize the research protocol for high accuracy and certainty of results.

ACKNOWLEDGEMENTS

Foundations: Supported by National Natural Science Foundation of China (No.82160195; No.82460203); Key R & D Program of Jiangxi Province (No.20223BBH80014).

Conflicts of Interest: Zhang H, None; **Xu ZS,** None; **Hu JY,** None; **Liu ZZ,** None; **Zhong L,** None; **He LQ,** None; **Chen C,** None; **Wang XY,** None; **Wei H,** None; **Zeng YM,** None; **Ling Q,** None; **Chen X,** None; **Wang YX,** None; **Shao Y,** None.

REFERENCES

1 Li K, Tian Y, Chen HB, *et al*. Temporal dynamic alterations of regional homogeneity in Parkinson's disease: a resting-state fMRI study. *Biomolecules* 2023;13(6):888.

2 Yu YJ, Liang RB, Yang QC, *et al*. Altered spontaneous brain activity patterns in patients after lasik surgery using amplitude of low-frequency fluctuation: a resting-state functional MRI study. *Neuropsychiatr Dis Treat* 2020;16:1907-1917.

3 Lu Q, Du Y, Zhang Y, *et al*. A genome-wide association study for susceptibility to axial length in highly myopic eyes. *Phenomics* 2023;3(3):255-267.

4 Du Y, Meng JQ, He WW, *et al*. Complications of high myopia: an update from clinical manifestations to underlying mechanisms. *Adv Ophthalmol Pract Res* 2024;4(3):156-163.

5 Landreneau JR, Hesemann NP, Cardonell MA. Review on the myopia pandemic: epidemiology, risk factors, and prevention. *Mo Med* 2021;118(2):156-163.

6 Eppenberger LS, Grzybowski A, Schmetterer L, *et al*. Myopia control: are we ready for an evidence based approach? *Ophthalmol Ther* 2024;13(6):1453-1477.

7 Rein DB, Lamuda PA, Wittenborn JS, *et al*. Vision impairment and blindness prevalence in the United States: variability of vision health responses across multiple national surveys. *Ophthalmology* 2021;128(1):15-27.

8 Williams KM, Verhoeven VJ, Cumberland P, *et al*. Prevalence of refractive error in Europe: the European eye epidemiology (E(3)) consortium. *Eur J Epidemiol* 2015;30(4):305-315.

9 Hansen MH, Hvid-Hansen A, Jacobsen N, *et al*. Myopia prevalence in

Denmark - a review of 140 years of myopia research. *Acta Ophthalmol* 2021;99(2):118-127.

10 Baird PN, Saw SM, Lanca C, *et al*. Myopia. *Nat Rev Dis Primers* 2020;6(1):99.

11 Midorikawa M, Mori K, Torii H, *et al*. Choroidal thinning in myopia is associated with axial elongation and severity of myopic maculopathy. *Sci Rep* 2024;14(1):17600.

12 Haarman AEG, Enthoven CA, Tideman JWL, *et al*. The complications of myopia: a review and meta-analysis. *Invest Ophthalmol Vis Sci* 2020;61(4):49.

13 Muma S, Naidoo KS, Hansraj R. Estimation of the lost productivity to the GDP and the national cost of correcting visual impairment from refractive error in Kenya. *PLoS One* 2024;19(3):e0300799.

14 Dong SS, Tian Q, Zhu TF, *et al*. SLC39A5 dysfunction impairs extracellular matrix synthesis in high myopia pathogenesis. *J Cell Mol Med* 2021;25(17):8432-8441.

15 Jones LA, Sinnott LT, Mutti DO, *et al*. Parental history of myopia, sports and outdoor activities, and future myopia. *Invest Ophthalmol Vis Sci* 2007;48(8):3524-3532.

16 Yu MK, Hu YY, Han M, *et al*. Global risk factor analysis of myopia onset in children: a systematic review and meta-analysis. *PLoS One* 2023;18(9):e0291470.

17 Martínez-Albert N, Bueno-Gimeno I, Gené-Sampedro A. Risk factors for myopia: a review. *J Clin Med* 2023;12(18):6062.

18 Tedja MS, Haarman AEG, Meester-Smoor MA, *et al*. IMI - myopia genetics report. *Invest Ophthalmol Vis Sci* 2019;60(3):M89-M105.

19 Pärssinen O, Kauppinen M. Associations of near work time, watching TV, outdoors time, and parents' myopia with myopia among school children based on 38-year-old historical data. *Acta Ophthalmol* 2022;100(2):e430-e438.

20 Seven I, Vahdati A, de Stefano VS, *et al*. Comparison of patient-specific computational modeling predictions and clinical outcomes of LASIK for myopia. *Invest Ophthalmol Vis Sci* 2016;57(14):6287-6297.

21 Murueta-Goyena A, Cañadas P. Visual outcomes and management after corneal refractive surgery: a review. *J Optom* 2018;11(2):121-129.

22 Tamimi A, Sheikhzadeh F, Ezabadi SG, *et al*. Post-LASIK dry eye disease: a comprehensive review of management and current treatment options. *Front Med* (*Lausanne*) 2023;10:1057685.

23 Shtein RM. Post-LASIK dry eye. *Expert Rev Ophthalmol* 2011;6(5):575-582.

24 Yu EY, Leung A, Rao S, *et al*. Effect of laser *in situ* keratomileusis on tear stability. *Ophthalmology* 2000;107(12):2131-2135.

25 Moshirfar M, Bhavsar UM, Durnford KM, *et al*. Neuropathic corneal pain following LASIK surgery: a retrospective case series. *Ophthalmol Ther* 2021;10(3):677-689.

26 Eydelman M, Hilmantel G, Tarver ME, *et al*. Symptoms and satisfaction of patients in the patient-reported outcomes with laser *in situ* keratomileusis (PROWL) studies. *JAMA Ophthalmol* 2017;135(1):13-22.

27 Sujanthan S, Shmuel A, Mendola JD. Resting-state functional MRI of the visual system for characterization of optic neuropathy. *Front Hum Neurosci* 2022;16:943618.

28 Huang X, Zhong YL, Zeng XJ, *et al*. Disturbed spontaneous brain activity pattern in patients with primary angle-closure glaucoma using amplitude of low-frequency fluctuation: a fMRI study. *Neuropsychiatr Dis Treat* 2015;11:1877-1883.

29 Min YL, Su T, Shu YQ, *et al*. Altered spontaneous brain activity patterns in strabismus with amblyopia patients using amplitude of low-frequency fluctuation: a resting-state fMRI study. *Neuropsychiatr Dis Treat* 2018;14:2351-2359.

30 Brown HD, Woodall RL, Kitching RE, *et al*. Using magnetic resonance imaging to assess visual deficits: a review. *Ophthalmic Physiol Opt* 2016;36(3):240-265.

31 Li Q, Huang X, Ye L, *et al*. Altered spontaneous brain activity pattern in patients with late monocular blindness in middle-age using amplitude of low-frequency fluctuation: a resting-state functional MRI study. *Clin Interv Aging* 2016;11:1773-1780.

32 Huang X, Zhou FQ, Hu YX, *et al*. Altered spontaneous brain activity pattern in patients with high myopia using amplitude of low-frequency fluctuation: a resting-state fMRI study. *Neuropsychiatr Dis Treat* 2016;12:2949-2956.

33 Li YX, Qin B, Chen Q, *et al*. Altered dynamic functional network connectivity within default mode network of epileptic children with generalized tonic-clonic seizures. *Epilepsy Res* 2022;184:106969.

34 Duncan ES, Small SL. Changes in dynamic resting state network connectivity following aphasia therapy. *Brain Imaging Behav* 2018;12(4):1141-1149.

35 Liu J, Liao XH, Xia MR, *et al*. Chronnectome fingerprinting: Identifying individuals and predicting higher cognitive functions using dynamic brain connectivity patterns. *Hum Brain Mapp* 2018;39(2):902-915.

36 Yao ZJ, Liao M, Hu T, *et al*. An effective method to identify adolescent generalized anxiety disorder by temporal features of dynamic functional connectivity. *Front Hum Neurosci* 2017;11:492.

37 Cui Q, Sheng W, Chen YY, *et al*. Dynamic changes of amplitude of low-frequency fluctuations in patients with generalized anxiety disorder. *Hum Brain Mapp* 2020;41(6):1667-1676.

38 Vergun S, Deshpande AS, Meier TB, *et al*. Characterizing functional connectivity differences in aging adults using machine learning on resting state fMRI data. *Front Comput Neurosci* 2013;7:38.

39 Ben-Hur A, Weston J. A user's guide to support vector machines. *Methods Mol Biol* 2010;609:223-239.

40 Meier TB, Desphande AS, Vergun S, *et al*. Support vector machine classification and characterization of age-related reorganization of functional brain networks. *Neuroimage* 2012;60(1):601-613.

41 Li T, Liao ZL, Mao YP, *et al*. Temporal dynamic changes of intrinsic brain activity in Alzheimer's disease and mild cognitive impairment patients: a resting-state functional magnetic resonance imaging study. *Ann Transl Med* 2021;9(1):63.

42 Zalesky A, Breakspear M. Towards a statistical test for functional connectivity dynamics. *Neuroimage* 2015;114:466-470.

43 Malecaze FJ, Boulanouar KA, Demonet JF, *et al*. Abnormal activation in the visual cortex after corneal refractive surgery for myopia: demonstration by functional magnetic resonance imaging. *Ophthalmology* 2001;108(12):2213-2218.

44 Vuori E, Vanni S, Henriksson L, *et al*. Refractive surgery in anisometropic adult patients induce plastic changes in primary visual cortex. *Acta Ophthalmol* 2012;90(7):669-676.

45 Hu YX, He JR, Yang B, *et al*. Abnormal resting-state functional network centrality in patients with high myopia: evidence from a voxel-wise degree centrality analysis. *Int J Ophthalmol* 2018;11(11): 1814-1820.

46 Zhai LY, Li Q, Wang TY, *et al*. Altered functional connectivity density in high myopia. *Behav Brain Res* 2016;303:85-92.

47 Guo MX, Dong HH, Zhang YT, *et al*. ALFF changes in brain areas of human with high myopia revealed by resting-state functional MRI. *2010 3rd International Conference on Biomedical Engineering and Informatics*. October 16-18, 2010, Yantai, China. IEEE, 2010:91-94.

48 Chen Y, Xiang CQ, Liu WF, *et al*. Application of amplitude of low-frequency fluctuation to altered spontaneous neuronal activity in classical trigeminal neuralgia patients: a resting-state functional MRI study. *Mol Med Rep* 2019;20(2):1707-1715.

49 Binkofski F, Fink GR, Geyer S, *et al*. Neural activity in human primary motor cortex areas 4a and 4p is modulated differentially by attention to action. *J Neurophysiol* 2002;88(1):514-519.

50 Guigon E, Baraduc P, Desmurget M. Coding of movement- and force-related information in primate primary motor cortex: a computational approach. *Eur J Neurosci* 2007;26(1):250-260.

51 Kim JA, Eliassen JC, Sanes JN. Movement quantity and frequency coding in human motor areas. *J Neurophysiol* 2005;94(4):2504-2511.

52 Hebant B, Costentin G, Slama M, *et al*. Precentral gyrus infarct presenting as isolated contralateral peripheral-type facial palsy. *Neurology* 2018;91(9):421-422.

53 Tokida H, Shiga, Shimoe Y, *et al*. Foreign accent syndrome caused by the left precentral infarction-a case report. *Clin Neurol* 2017;57(6): 293-297.

54 Mori E, Yamadori A, Furumoto M. Left precentral gyrus and Broca's aphasia: a clinicopathologic study. *Neurology* 1989;39(1):51-54.

55 Chauhan P, Rathawa A, Jethwa K, *et al*. The Anatomy of the Cerebral Cortex. In: Pluta R, editor. *Cerebral Ischemia*. 2021. Chapter 1.

56 Uddin LQ, Nomi JS, Hébert-Seropian B, *et al*. Structure and function of the human insula. *J Clin Neurophysiol* 2017;34(4):300-306.

57 Zinn PO, Habib A, Deng H, *et al*. Uncovering interoceptive human insular lobe function through intraoperative cortical stimulation-a review. *Brain Sci* 2024;14(7):646.

58 Ferreira MA. Neuroanatomy Applied to Clinical Practice. *Fundamentals of Neurosurgery: A Guide for Clinicians and Medical Students.* Springer 2019:1-23.

59 Centanni SW, Janes AC, Haggerty DL, *et al*. Better living through understanding the insula: why subregions can make all the difference. *Neuropharmacology* 2021;198:108765.

60 Lamm C, Singer T. The role of anterior insular cortex in social emotions. *Brain Struct Funct* 2010;214(5-6):579-591.

61 Molnar-Szakacs I, Uddin LQ. Anterior insula as a gatekeeper of executive control. *Neurosci Biobehav Rev* 2022;139:104736.

62 De Raedt S, De Vos A, de Keyser J. Autonomic dysfunction in acute ischemic stroke: an underexplored therapeutic area? *J Neurol Sci* 2015;348(1-2):24-34.

63 Oppenheimer S. Cerebrogenic cardiac arrhythmias: cortical lateralization and clinical significance. *Clin Auton Res* 2006;16(1):6-11.

64 Bud Craig AD. Forebrain emotional asymmetry: a neuroanatomical basis? *Trends Cogn Sci* 2005;9(12):566-571.

65 Nagai M, Kishi K, Kato S. Insular cortex and neuropsychiatric disorders: a review of recent literature. *Eur Psychiatry* 2007;22(6):387-394.

66 Li JY, Kuang SR, Liu Y, *et al*. Structural and functional brain alterations in subthreshold depression: a multimodal coordinate-based meta-analysis. *Hum Brain Mapp* 2024;45(7):e26702.

67 Lanzenberger R, Baldinger P, Hahn A, *et al*. Global decrease of serotonin-1A receptor binding after electroconvulsive therapy in major depression measured by PET. *Mol Psychiatry* 2013;18(1):93-100.

68 Su L, Cai YY, Xu YF, *et al*. Cerebral metabolism in major depressive disorder: a voxel-based meta-analysis of positron emission tomography studies. *BMC Psychiatry* 2014;14:321.